Creep Recovery of Acrylate Urethane Oligomer/Acrylate Networks

K. KAWATE,* T. SASAKI, and G. ELLIOTT

Sumitomo 3M Limited, 8-8, Minami-Hashimoto 3-chome, Sagamihara City, Kanagawa-Pref., 229, Japan

SYNOPSIS

Creep recovery of acrylate urethane/acrylate networks was investigated as a function of time and temperature. An important outcome was the capacity for superimposition of experimental data obtained at various temperatures. Arrhenius type temperature dependence of the creep recovery was also observed. The master curve obtained did not significantly depend on the measuring mode of creep recovery or the crosslink density, and the response could be approximated by the Bueche theory. The dynamic mechanical properties of the systems were also investigated. Retardation spectrum L obtained from the dynamic mechanical data overlapped with that obtained from the creep recovery data. The activation energy obtained from the temperature dependence of the shift factor a_T also agreed with that obtained from the temperature dependence of the creep recovery. © 1996 John Wiley & Sons, Inc.

INTRODUCTION

Homopolymers in the temperatures range slightly below their own glass transition temperatures, or block copolymers consisting of flexible chain and rigid chain are usually deformable to a great extent. However, the recovery from the deformation spends very long time and can be sometimes regarded as a "permanent deformation." The recovery process is drastically accelated by heating when the temperature dependence of the recovery process is large and it is complete when those polymers are chemically or physically crosslinked to prevent irreversible flow. Some authors define such phenomena as "shape memory" and call those polymers described above as "shape memory polymers." The polymers have been recently used for medical materials, dental materials, toys and clothes.[1-5]

This shape memory phenomena may be described by creep recovery experiments from the rheological point of view.[6] Despite the fact that many creep experiments for crosslinked polymer have been described,[7-15] creep recovery experiments have seldom been reported,[16] perhaps due to experimental difficulty involving irreversible flow, crystallization, or destruction of materials. Creep recovery experiments for shape memory polymers have not been reported either. On the other hand, creep recovery of uncrosslinked polymers has been widely investigated in terms of dimensional instabilities.[17-20]

According to Boltzmann superposition principle,[6,21] the shear creep compliance $J(t)$ measured in the time period $0 < t < t_1$ is equal to the recovered creep compliance $J_r(t')$ for $t > t_1$ with the new time scale $t' = t - t_1$ for a crosslinked material.

Within the framework of linear viscoelastic theory, shear creep compliance $J(t)$ relates to retardation spectra L, which is interrelated to the relaxation spectra H obtained from dynamic mechanical data. Because dynamic mechanical analysis is a popular and sophisticated technology, it may offer a very convenient means of predicting creep recovery behavior.

In the present study, we report on the creep recovery and the dynamic mechanical properties obtained for acrylate urethane oligomer/acrylate networks. The radiation cured systems of acrylate urethane oligomer and monofunctional acrylate covered a variety of mechanical properties ranging from very strong to very elastic.[22] In addition, the combinations

* To whom correspondence should be addressed.

Journal of Applied Polymer Science, Vol. 61, 1413-1421 (1996)
 CCC 0021-8995/96/081413-09

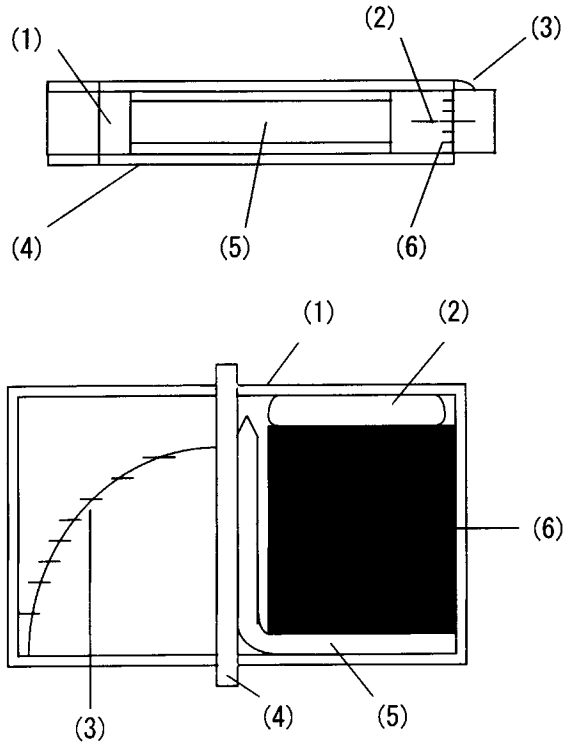

Figure 1 (a) Apparatus for torsioning creep recovery: (1) plastic rod, (2) mark, (3) adhesive tape, (4) plastic tube, (5) sample, (6) scale. (b) Apparatus for bending creep recovery: (1) plastic box, (2) wedge, (3) scale, (4) peg, (5) sample, (6) bending support block.

of flexible oligomers and high T_g acrylates yielded shape memory behaviors around room temperature. Because those were crosslinked systems, experimental difficulty owing to the flow under stress was negligible.

EXPERIMENTAL

Materials and Sample Preparation

Acrylated urethane prepolymers used were reaction products of polyols of diverse composition with diisocyantes, and then the terminal isocyanate groups were treated with 2-hydroxyethyl acrylate or methacrylate.[23] In this study, commercially available urethane acrylate UX4101 (Kayarad, Nippon Kayaku Co., Ltd.) based on aliphatic diisocyante with acrylate groups at each end was used as received. The weight average molecular weight of UX4101 was 6700 ± 600 according to the supplier's data analysis.

The urethane adduct of 2 : 1 2-hydroxyethylacrylate reacted with isophorondiisocyanate (IA) was obtained from Sanwa Chemical Industry Co., Ltd.

t-Butylacrylate (tBA) and methylmethacrylate (MMA) were obtained from Wako Pure Chemical Industries. Ltd.

Isobornyl acrylate (IBA) was obtained from Kyoeisha Chemical Co., Ltd.

The radical photo initiator 2-hydroxy-2-methyl-1-phenylpropan-1-one (D1173) was obtained from Ciba-Geigy.

Samples of composition (A): UX4101/tBA/D1173 = 60/40/1, (B): UX4101/IA/tBA/D1173 = 40/20/40/1, (C): UX4101/IBA/D1173 = 60/40/1 and (D): UX4101/MMA/D1173 = 60/40/1 (parts by weight), were prepared by addition and mixing at 50°C followed by UV-curing between PET films, utilizing a 4 mm silicon rubber mold. Curing was achieved by exposure to a 300 W high pressure mercury vapor lamp (HSL-300/13-FM, ORC Manufacturing Co., Ltd.). The distance between the lamp and sample was 30 cm and the irradiation time was 60 min.

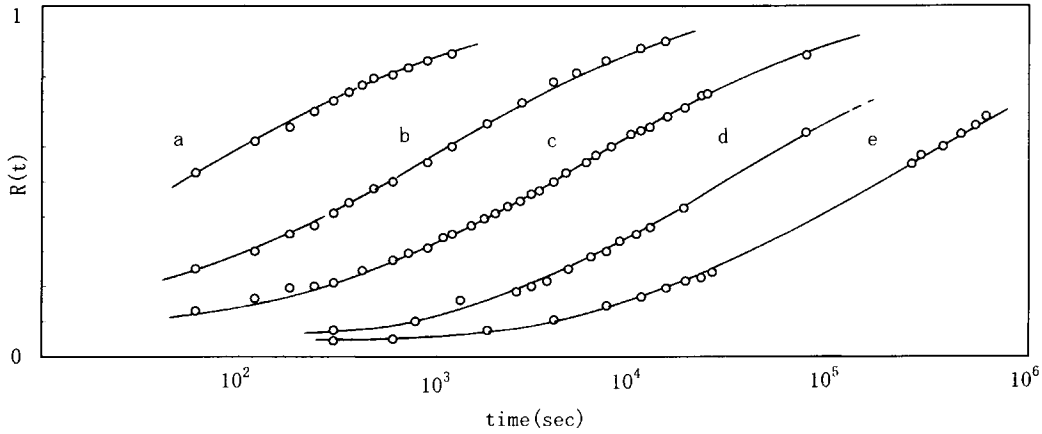

Figure 2 Torsioning creep recovery was measured vs. time at various temperatures for sample A. The curves a, b, c, d, and e were obtained at 25, 15, 10, and 5°C, respectively.

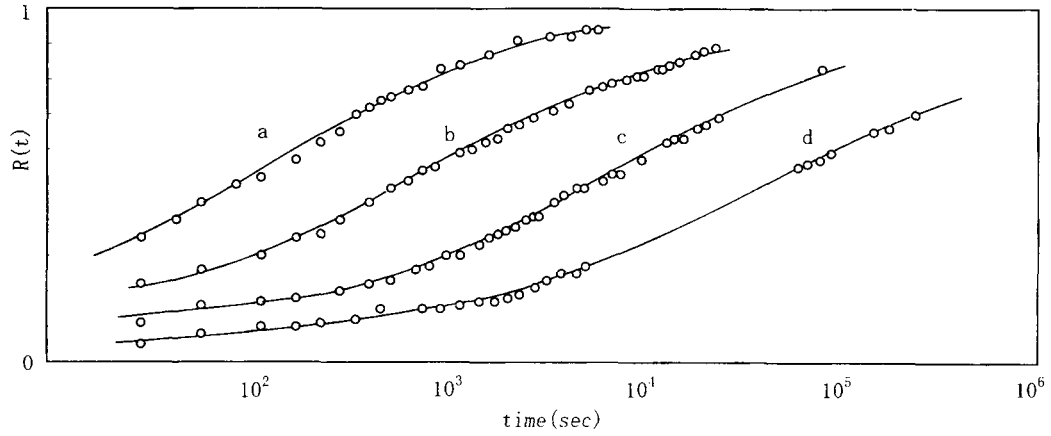

Figure 3 Torsioning creep recovery was measured vs. time at various temperatures for sample B. The curves a, b, c, and d were obtained at 55, 50, 45, and 40°C, respectively.

The creep samples were formed as rectangular parallelepiped bar with a cross section of 6.0 × 4.0 mm^2 and length in 40 mm.

Torsioning Creep Recovery Measurements

Depicted in Figure 1(a) is the apparatus devised for measuring creep recovery via torsioning mode. Both ends of the rectangular bar sample were adhered to a plastic rod of 10 mm diameter, 18 mm length. This unit was inserted into a plastic tube of 10.5 mm inside diameter, 60 mm length. One of the rods was adhered to the tube, whereas the other was temporarily fixed in a torsion position using adhesive tape. The initial torsion position θ_0 was 180° for sample A and 90° for sample B. Samples A and B fixed in a torsion position were heat treated at 65 and 90°C, respectively, for 10 min. After the heat treatment, the apparatus was put into glass tube of 14 mm inside diameter immersed in a thermostated water bath. The apparatus was kept at analysis temperature for 40 min for thermal equilibration. Torsioning recovery was initiated by the removal of the adhesive tape and torsioning angle θ was subsequently measured as a function of time t. The torsioning recovery $R(t)$ was defined as

$$R(t) = (\theta_0 - \theta(t))/\theta_0 \quad (1)$$

Bending Creep Recovery Measurements

Depicted in Figure 1(b) is a bending mode apparatus. The casing was a plastic box with dimensions 30 × 60 × 15 mm^3. The pegging device temporary held the sample in a bent position of 90° around 25 × 25 mm plastic block until creep recovery was initiated by the removal of this peg. After the heat treatment

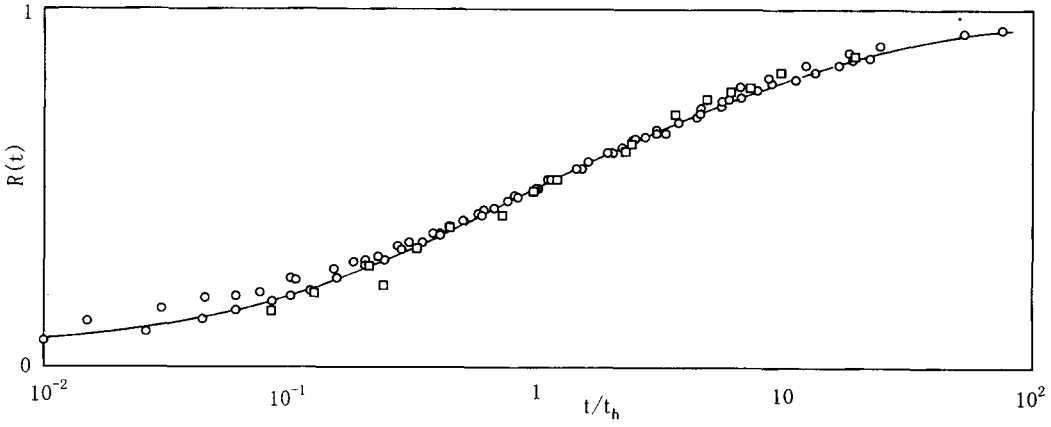

Figure 4 The torsioning creep recovery (○) and bending creep recovery (□) at several temperatures for sample A are plotted against t/t_h.

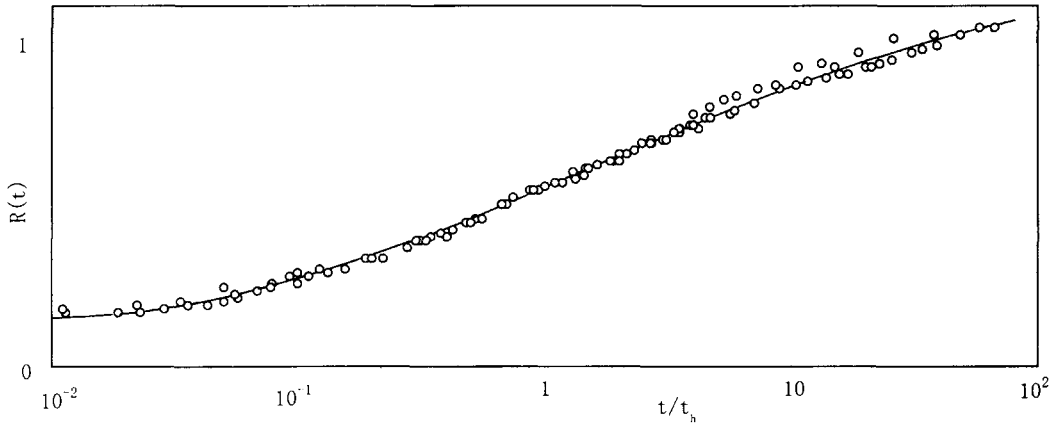

Figure 5 The torsioning creep recovery at several temperatures for sample B are plotted against t/t_h.

and thermal equilibrium described above, the peg was removed. The bent angle θ was measured as a function of time t. The bending recovery was also defined as eq. (1).

Dynamic Mechanical Measurements

The complex shear moduli, $G^* = G' + iG''$ were obtained with a Rheometrics Dynamic Analyzer RDA-II. The torsioning test was carried out using rectangular bars with a cross-sections 12.8 × 3.4 mm and lengths between the clamps of 25.0 mm with 0.5% strain in the frequency range from 0.1 to 100 rad/s. The glass transition temperature T_g was defined as the temperature of maximum tan $\delta = G''/G'$ when the temperature was raised by step for every 5 min at 6.28 rad/s. The crosslink density N_v, for instance, the molar concentration of network chains, was calculated from G' at 100°C using the equation

$$N_v = G'/RT \tag{2}$$

where RT is the usual meaning.

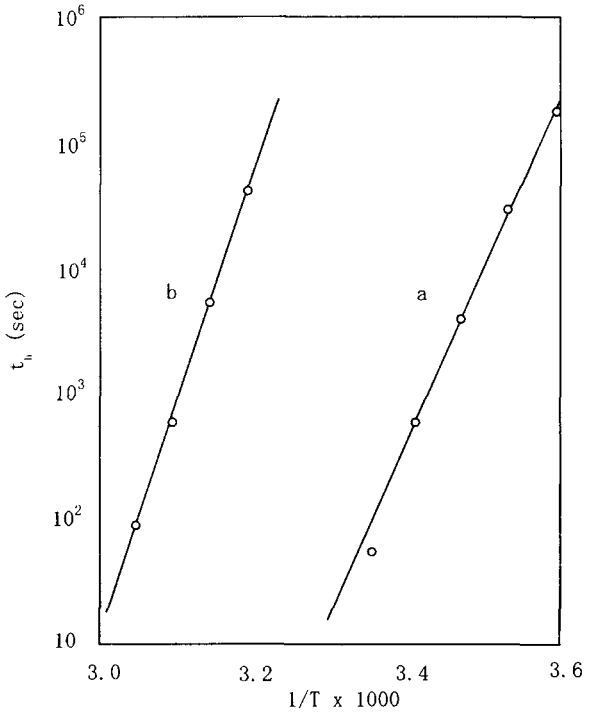

Figure 6 Logarithms of 50% creep recovery time t_h are plotted against inverse absolute temperatures. The lines a and b were obtained from sample A and sample B.

RESULTS

The torsioning creep recovery data of sample A and B are shown in Figures 2 and 3, respectively. Because the creep recovery curves were similar in form, the data was replotted as a function of reduced time t/t_h as shown in Figures 4 and 5. Here, t_h is the 50% creep recovery time at each temperature. In Figure 4, the bending creep recovery data of sample A were also plotted.

In Figure 6, logarithms of t_h were plotted against inverse absolute temperatures. The temperature dependence of t_h demonstrated Arrhenius-type behavior

$$t_h = t_h^0 exp(E_a/RT) \tag{3}$$

where E_a is the activation energy of creep recovery. The activation energy of sample A and B were determined from the plot as 66 and 87 kcal/mol, respectively.

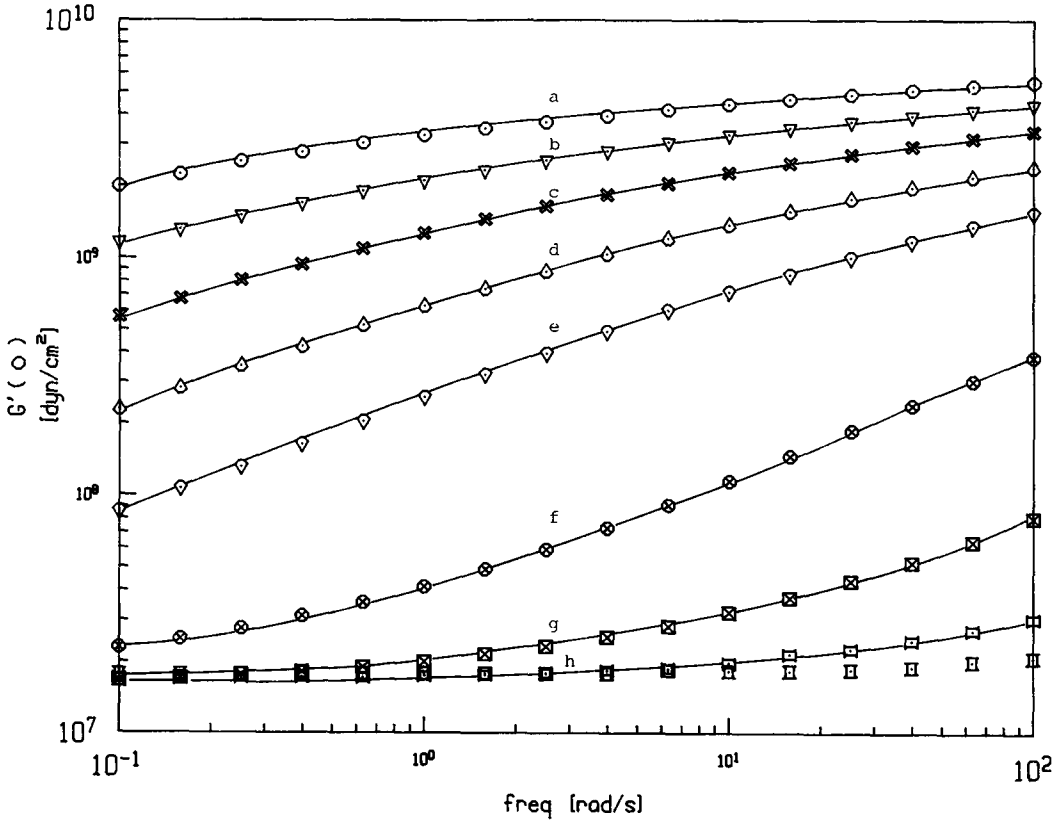

Figure 7 Storage mdoulus G' of sample A plotted logarithmically against angular frequency at eight temperatures. The curves a, b, c, d, e, f, g, and h were obtained at 3.6, 8.8, 13.6, 18.7, 23.6, 34.0, 44.2, and 54.4°C, respectively.

In Figure 7, storage shear modulus G' of sample A was plotted against angular frequency. In Figure 8, the master curve obtained by shifting G' in Figure 7 to 23.6°C and the other master curve obtained by shifting corresponding G'' to 23.6°C are shown. Below T_g, the temperature dependence of shift factor a_T is allowed an equation of the Arrhenius form as shown in Figure 9, with E_a = 67 kcal/mol, which agreed with that obtained from the creep recovery measurements. Good agreement was also obtained for sample B, as shown in Table I. The temperature dependence of the shift factor above T_g seemed to deviate from the Arrhenius equation. In Table I, the activation energies of the other two systems, as determined from the temperature dependence of the shift factor are listed.

DISCUSSION

Retardation Spectrum and Relaxation Spectrum

Within the framework of linear viscoelastic theory, retardation spectrum L of retardation time τ is defined by the equation

$$J(t) = \int_{-\infty}^{\infty} L(\tau)[1 - \exp(-t/\tau)]\, d \ln \tau + t/\eta_0 \tag{4}$$

where $J(t)$ is compliance, η_0 is steady-state viscosity.[6] Therefore, creep recovery $R(t)$ is expressed by the spectrum L for the crosslinked polymer as

$$R(t) = A \int_{-\infty}^{\infty} L(\tau)[1 - \exp(-t/\tau)]\, d \ln \tau \tag{5}$$

where the coefficient A is determined from the experimental condition $R(\infty) = 1$ meaning completely recovery from deformation. Therefore, A is calculated as

$$A = \left[\int_{-\infty}^{\infty} L(\tau)\, d \ln \tau\right]^{-1} = 1/J(t{=}\infty) = G'(w = 0) \tag{6}$$

In order to determine L from creep data, we use approximation[24]

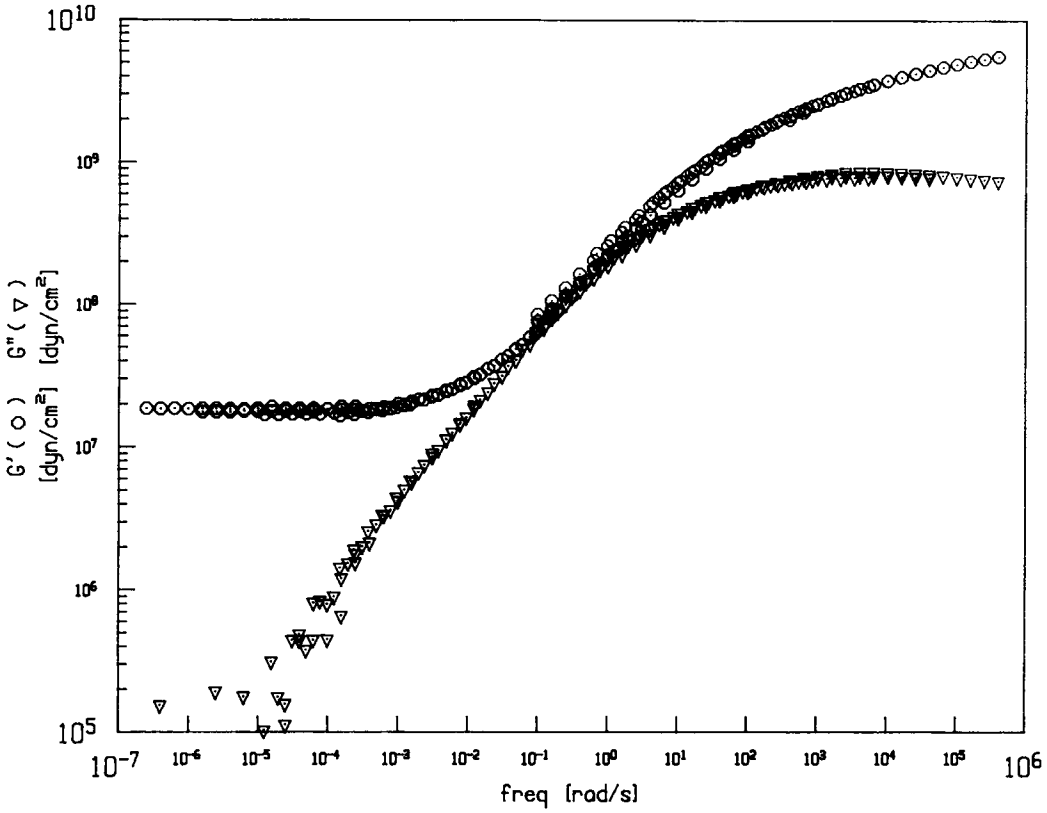

Figure 8 Master curves obtained by plotting the data of G' in Figure 7 and G'' with reduced variables, representing the behavior over an extended frequency scale at reference temperature T_o = 23.6°C.

$$L(\tau) = 1/AdR(t)/d(\ln t)|_{t=\tau} \qquad (7)$$

Relaxation spectrum H of relaxation time τ is defined by the equation

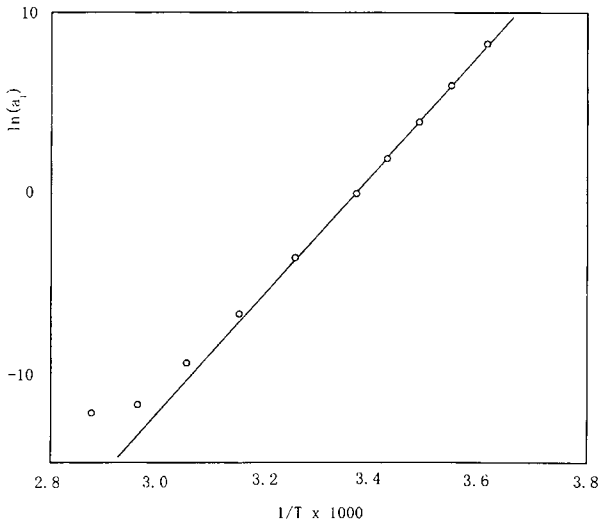

Figure 9 The temperature dependence of the shift factor a_T used in plotting Figure 8.

$$G(t) = \int_{-\infty}^{\infty} H(\tau)\exp(-t/\tau)\, d\ln\tau + G_e \qquad (8)$$

where $G(t)$ is modulus, G_e is equilibrium modulus.[6] Shear storage modulus G' and shear loss modulus G'' are expressed by the spectrum H as

$$G'(w) = \int_{-\infty}^{\infty} H(\tau)w^2\tau^2/(1 + w^2\tau^2)\, d(\ln\tau) \qquad (9a)$$

$$G''(w) = \int_{-\infty}^{\infty} H(\tau)w\tau/(1 + w^2\tau^2)\, d(\ln\tau) \qquad (9b)$$

Where w is the measuring frequency in radius per second. In order to determine H from dynamic mechanical data, we use approximation[24]

$$H(\tau) = dG'(w)/d(\ln w)|_{\tau=1/2\pi w} \qquad (10)$$

Retardation spectrum L is calculated from G', G'' and H by the relation according to Ferry[6]

Table I Glass Transition Temperature, Activation Energy of Creep, and Crosslink Density

System	T_g (°C)	E_a (Creep) (kcal/mol)	E_a (a_T) (kcal/mol)	N_v (mol/cm^3)
A	34	66	67	7×10^{-4}
B	70	88	87	1×10^{-3}
C	55	—	67	8×10^{-4}
D	54	—	66	8×10^{-4}

$$L(\tau) = H(\tau)/\{[G' - G'' + 1.37H(\tau)]^2 + \pi^2 H^2\} \quad (11)$$

In Figure 10, retardation spectrum L and relaxation spectrum H obtained from dynamic mechanical measurements were determined using eqs. (10) and (11) and plotted against angular frequency. L obtained from creep recovery measurements using eq. (7) with $A = 2 \times 10^7$ was plotted against $w = 1/(2\pi\tau)$ represented by a dotted line in Figure 10.

Comparison with Bueche Theory

According to the Bueche theory,[25] a very low crosslinked elastomeric network wherein each chain is linked directly to only two other chains is expected to reach an equilibrium deformation soon after a constant load has been applied to it. Such networks show a narrow retardation spectrum and, consequently, the creep recovery will occur rapidly. The creep recovery of those networks can be written as

$$R(t) = \frac{\sum 1/n^2[1 - \exp(-n^2 t/\tau)]}{\sum 1/n^2} \qquad n = 1, 3, 5 \cdots \infty \quad (12)$$

The creep recovery calculated from eq. (12) is represented as a chain curve in Figure 11.

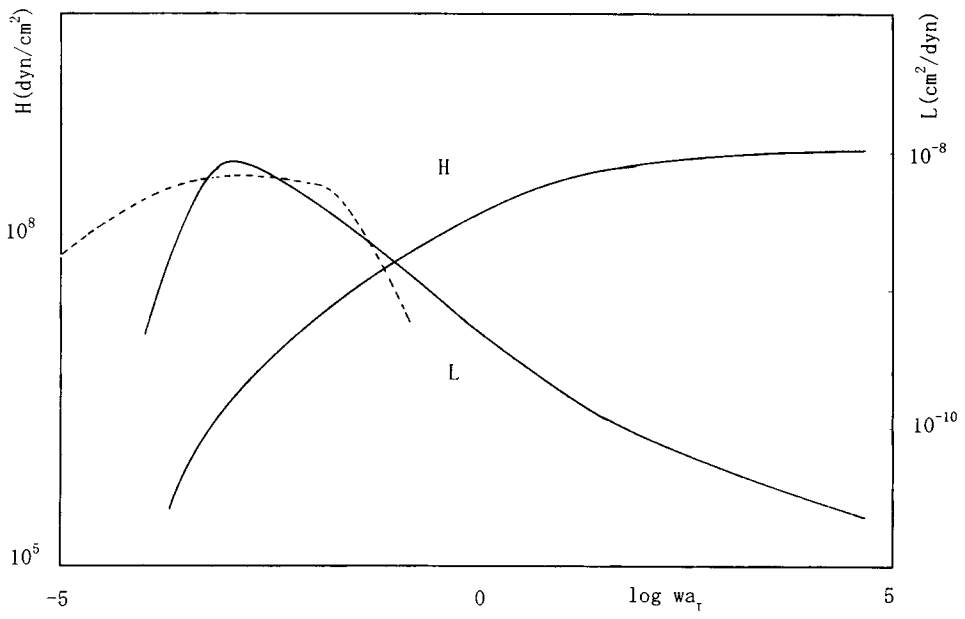

Figure 10 The relaxation spectrum H and the retardation spectrum L for sample A reduced to 23.6°C. The solid curves H and L were obtained from dynamic mechanical measurements with eqs. (10) and (11). The dotted curve was obtained from creep recovery data with eq. (7) for A = 2×10^7.

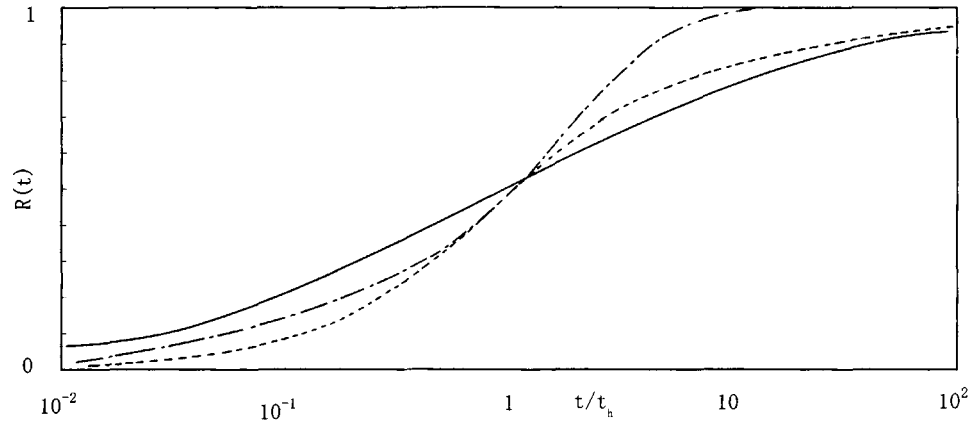

Figure 11 Master curve for creep recovery. The solid curve represents experimental data for sample A. The chain curve is calculated from eq. (12). The dotted curves are calculated from eq. (13) for $\beta = 3$ and 2, respectively.

On the other hand, a more highly crosslinked network will behave somewhat more sluggishly because of the larger friction associated with many chains linked to one chain. The creep recovery of such networks is given by

$$R(t) = \frac{1 - \exp(-t/\tau) + \sum \beta^{-n}[1 - \exp(-t/\tau\beta^{2n})]}{1 + \sum \beta^{-n}}$$

$$n = 1, 2, 3, \cdots \infty \qquad (13)$$

where β is the number of chains issuing from the one end of the chain. The creep recovery calculated from eq. (13) is represented as dotted curves in Figure 11. Equation (13) with $\beta = 2$ provides a fairly good explanation of experimental creep recovery behavior.

CONCLUSION

Creep recovery of acrylate urethane oligomer/acrylate networks was measured by torsioning and bending experiments. When creep recovery data measured at various temperature were plotted vs. a reduced time variable t/t_h, the master curve was obtained. The functional form of the master curve did not significantly depend on measuring mode or crosslink density and was approximately representable by Bueche theory. Retardation spectrum obtained from the creep recovery data was overlapped with that obtained from dynamic mechanical measurements. The activation energy obtained from the temperature dependence of t_h also agreed with that obtained from the temperature dependence of the shift factor a_T. These results indicate that the shape memory of acrylate urethane oligomer/acrylate networks is identical with the creep recovery within the framework of linear viscoelastic theory. The time–temperature superposition allows the accurate determination of the creep recovery at very long time. For example, the time required to 80% creep recovery of sample A at 0°C is calculated as 230 days. Because the creep recovery of the present systems is exactly determinable, it would be applicable to functional materials.

REFERENCES

1. N. Nagata, *Kagaku,* **45**(8), 554 (1990).
2. H. Tobushi, S. Hayashi, and P. Lin, *Nippon Kikai Gakkai Ronbunshu,* Part A, **60**(575), 1676 (1994).
3. S. Minatono, M. Ishii, and K. Wada, *JETI,* **36**(7), 179 (1988).
4. M. Karoji and A. Hirata, *Plastic,* **40**(2), 49 (1986).
5. A. Hirata, *Koubunshi,* **38,** 843 (1989).
6. J. D. Ferry, *Viscoelastic Properties of Polymers,* John Wiley, New York, 1980.
7. E. Maekawa, R. G. Mancke, and J. D. Ferry, *J. Phys. Chem.,* **69,** 2811 (1965).
8. N. R. Langley, *Macromolecules,* **1,** 348 (1968).
9. R. A. Dickie and J. D. Ferry, *J. Phys. Chem.,* **70,** 2594 (1966).
10. J. F. Sanders and J. D. Ferry, *Macromolecules,* **7,** 681 (1974).
11. D. J. Plazek, *J. Polym. Sci., A-2,* **4,** 745 (1966).
12. L. H. Sperling and A. V. Tobolsky, *J. Polym. Sci., A-2,* **6,** 259 (1968).

13. L. E. Nielsen, *J. Appl. Polym. Sci.*, **8,** 511 (1964).
14. E. D. Farlie, *J. Appl. Polym. Sci.*, **14,** 1127 (1970).
15. M. H. Wagner and S. E. Stephenson, *J. Rheol.*, **23,** 489 (1979).
16. F. S. Conant, G. L. Hall, and W. J. Lyons, *J. Appl. Phys.*, **21,** 499 (1950).
17. K. van Holde, *J. Polym. Sci.*, **24,** 417 (1957).
18. G. C. Berry, *J. Polym. Sci. Phys.*, **14,** 451 (1976).
19. L. C. E. Struik, *Internal Stress, Dimentional Instabilities and Molecular Orientations in Plastics,* John Wiley & Sons, New York, 1990.
20. H. Gramerspacher and J. Meissner, *J. Rheol.*, **39,** 151 (1995).
21. L. Boltzmann, *Pogg Ann. Erg.*, **7,** 624 (1876).
22. K. Kawate and T. Sasaki, *Polym. Bull.*, **27,** 213 (1991).
23. S. P. Pappas, Ed., *UV-Curing: Science and Technology,* Chap. 4, Technology Marketing Corporation, Norwalk, CN, 1985.
24. F. Bueche, *Physical Properties of Polymers,* Chap. 7, John Wiley, New York, 1962.
25. F. Bueche, *J. Appl. Polym. Sci.*, **1,** 240 (1959).

Received September 18, 1995
Accepted February 17, 1996